P-7-20

Extended Abstracts of the 2010 International Conference on Solid State Devices and Materials, Tokyo, 2010, pp423-424

Mach-Zehnder Electro-Optic Modulator Fabricated on Silicon-on-Insulator (SOI) Substrate Based on the Multimode Interference (MMI) Effect

Ricky W. Chuang[a,c*], Mao-Teng Hsu[a], Yu-Chun Chang[a], Shen-Horng Chou[c], and Yao-Jen Lee[b]

[a]Institute of Microelectronics, Department of Electrical Engineering, Advanced Optoelectronic Technology Center (AOTC), and Center for Micro/Nano Science and Technology, National Cheng Kung University, Tainan 70101, Taiwan, R.O.C.
[b]National Nano Device Laboratories, Hsinchu City 30078, Taiwan, R.O.C.
[c]National Nano Device Laboratories, Tainan 74147, Taiwan, R.O.C.
[*]Corresponding Author's Phone and Email: +886-6-2757575 ext. 62397 and rwchuang@mail.ncku.edu.tw

INTRODUCTION

Silicon photonics have spurred a growing interest in recent years, mainly because of its unique applicability in optical interconnects [1-2] which are considered as a promising alternative to replace conventional electrical interconnects Using photons in place of electrons to transmit digital information over the long links is deemed helpful for achieving high bandwidth, low power consumption, low noise, data transfer with minimal crosstalk and high interconnection density. In addition, implementing efficient optical functions in Si would allow us to take advantages of the mature and low cost silicon CMOS technology for the fabrication of monolithic micro-photonics circuits. The impetus for investigating silicon photonics primarily comes from the ultimate needs of integrating optical and electrical devices on the same substrate, so-called the optoelectronic integrated circuits (OEICs). The monolithic integration is expected to find many system applications when miniaturization and costs are of major concerns.

One of most important functions often performed by the integrated optics devices is to realize multi-direction optical beam splitting and combining. Guided-wave devices based on multimode interference (MMI) effects fulfill the above requirements, owing to their reasonable bandwidth, compact size, high fabrication tolerances and good power balance. They have been widely used in various integrated optical circuits for realizing multi-directional optical beam splitting with high accuracy and low loss in short propagation length [3-4]. MMI devices are functionally based on the principle of self-imaging, which was first proposed by Bryngdahl *et al.* [5] and later elucidated in more detail by Ulrich [6]. The operation principle of MMI devices involves the phenomenon of interference between modal fields in multimode waveguide. With regards to our approach to the design of the MMI-MZIs, we wish to emphasize that our proposed MZIs based on the MMI effect would benefit from the significant reductions of the waveguide scattering and radiation losses as the S-bends and Y-branches are not used for the design of MZIs. Furthermore, MMI-MZIs with the three different phase shifter lengths of 460, 960, and 1960 μm were designed, fabricated, and thoroughly analyzed. The corresponding experimental results will be shown hereafter.

EXPERIMENTS

Figure 1(a) shows a diagram of top view of our 1×2 MMI-based MZI modulator. It consists of three components: a 3-dB power splitter, a phase shifter, and a 2×1 3-dB power combiner. The input, output, and delay lines for MZI have waveguide width W = 10 μm. The distance between two arms is 10 μm. The power splitter and power combiner are designed with the same size; their length and width are described as L_{MMI} (~1930 μm) and W_{eq} (40 μm), respectively. The cross-sectional view of 1×2 MMI-based MZI modulator with a phase shifter is shown in Fig. 1(b). At first, a highly-doped N^+ silicon substrate with the concentration of around 1×10^{20} cm^{-3} was used as the lower cladding layer. The silicon-on-silicon (SOS) wafer was evaluated by using the spreading resistance profiling (SRP) system to determine the relation of the doping

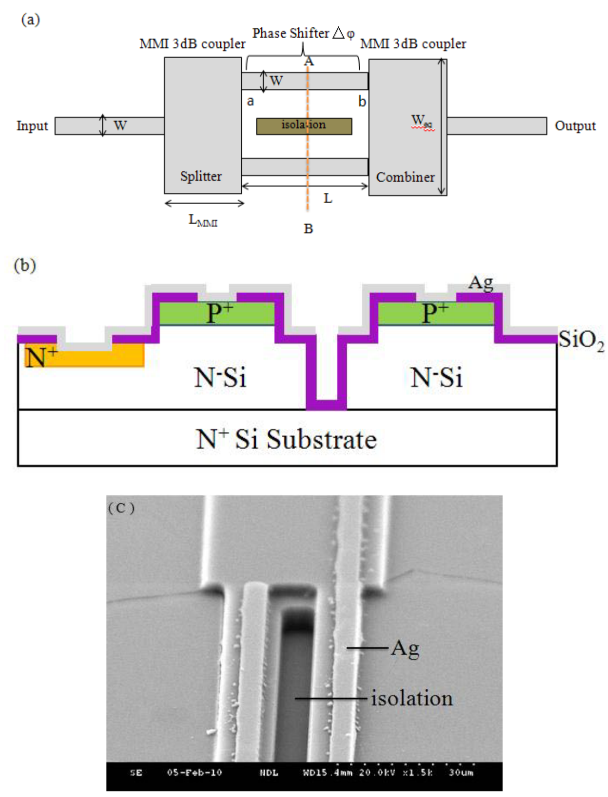

FIG. 1. (a) Schematic diagram of a MZI modulator composed of two 1 × 2 multimode interference (MMI) sections cascaded in a back-to-back fashion. (b) The cut line AB illustrated in Fig. 1(a) reveals a cross section of a modulator with a phase shifter. (c) Scanning electron microscope (SEM) image of the MMI-based MZI modulator.

concentration versus depth (not shown). The thickness of N^--silicon epitaxial layer (10^{15} cm^{-3}) is approximately 6 μm serving as a core layer. The refraction index contrast between epitaxial Si and substrate was estimated to be ~0.02 corresponding to *n*-type Si layer with a highly doped concentration of 1 × 10^{20} cm^{-3} at λ = 1.55 μm. Next, the lithography was used to define the N^+ and P^+ doping regions, before creating them with a spin-on-dopant (SOD) technique. The rib waveguide and isolation were etched by using Oxford Plasma 380 inductively-coupled plasma (ICP) etcher. The rib waveguide width and isolation depth etched were ~1.52 and 4.3 μm, respectively. The isolation was etched down to the N^+ substrate in order to prevent optical light from coupling into the other arm. Next, plasma-enhanced chemical vapor deposition (PECVD) chamber was used to deposit a 0.5 μm-thick SiO_2 layer in order to minimize the optical absorption by metal contacts. Finally, the Al/Ag bilayer films with thickness of 150/500 nm were deposited by DC sputter system. The optical measurements of our devices were performed on an optical bench equipped with a vibration isolation system. The incident light was launched and coupled into the input waveguide from a single mode fiber of a 1550 nm tunable laser and the output optical signal was monitored by a high-speed optical photoreceiver.

RESULTS AND DISCUSSION

The beam propagation method (BPM) was used to simulate the proposed MMI-based MZI modulator, from which the extinction ratio of approximately −18.3dB was determined. After the devices were fabricated, the modulation capability of MMI-MZIs was evaluated using Keithley 2612 dual-channel source meter and high-speed optical photoreceiver. One of the measurement results corresponding to MMI-MZIs with three different phase shifter lengths of 460, 960, and 1960 μm long are respectively depicted in Fig. 2(a), 2(b), and 2(c). According to Fig. 2, the first π phase shift occurs at a driving power of 0.2 W. Furthermore, the extinction ratios achieved for MMI-MZIs with three different modulation lengths is approximately −16.8, −21.2, and −18.9 dB, which corresponds to the modulation depths of ~97.8, 97,9 and 98.7%, respectively.

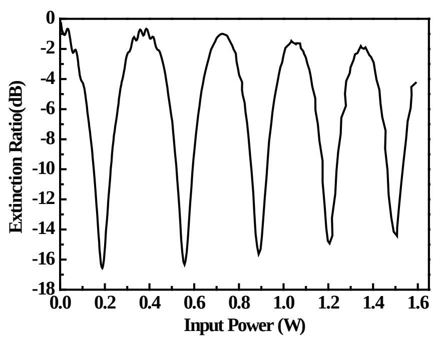

(a)

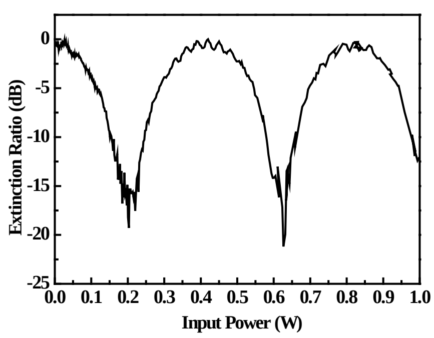

(b)

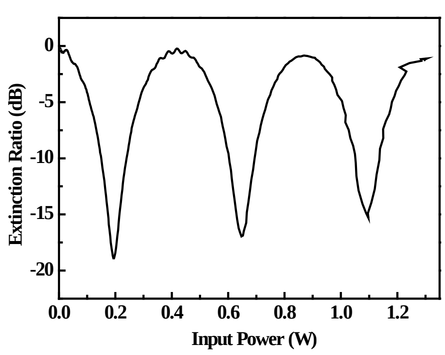

(c)

FIG. 2. The relationship between the driving power and the extinction ratio obtained for MMI-MZIs with the three different modulation lengths of (a) 460, (b) 960, and (c) 1960 μm.

The optical responses of the corresponding MMI-MZIs with the three different phase shifter lengths were also measured using a high-speed optical photoreceiver connected to an oscilloscope. A square wave voltage pulse with the frequency of 1 MHz and duty cycle of 50% was applied to one of the arms. As shown in Fig. 3(a) for MMI-MZI with the shifter length of 460 μm, the rise time defined as the times required for the signal amplitude to rise from 10 to 90% of the output maximum, was measured to be 56 ns, while the fall time defined as the time required for the signal amplitude to decay from 90 to 10% of output maximum, was also measured as 84 ns. Furthermore, the rise/fall times measured for other MMI-MZIs with the phase shifter lengths of 960 and 1960 μm were 52/84 ns and 76/88 ns, respectively.

CONCLUSIONS

In summary, the design of MMI-based 3dB MZI power splitter/combiner with dimensions of 6000 μm × 40 μm was proposed and analyzed. The operation of this device was based on the carrier injection effect, from which an approximate extinction ratio of −18.3 dB was obtained using BPM simulation. As for the device measurements, when the driving power was set at 0.2 W, the first π phase shift was observed. Finally, the optical response measurements indicated that the rise/fall times determined for MMI-MZIs with the three different modulation lengths of 460, 960, and 1960 μm were 56/84 ns, 52/84 ns, and 76/88 ns, respectively. The detailed device fabrication steps and the corresponding measurement results will be reported during the upcoming SSDM 2010 conference.

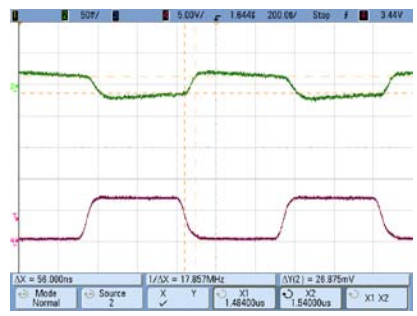

(a)

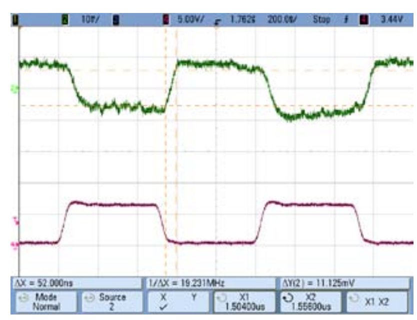

(b)

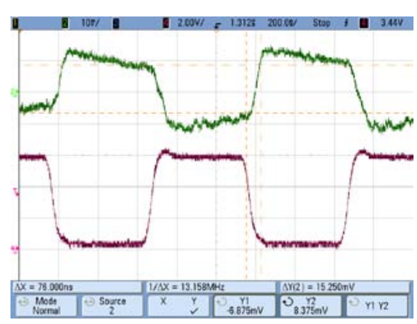

(c)

FIG. 3. Optical modulation characteristics of MMI-MZIs with the three different modulation lengths of (a) 460, (b) 960, and (c) 1960 μm, measured in response to a square wave voltage pulse applied. The upper and lower waveforms correspond to the light signal detected by the photoreceiver and the input electrical pulse with the frequency of 1 MHz applied to the device, respectively.

REFERENCES

[1] R. A. Soref, “Silicon-based optoelectronics,” *Proc. IEEE*, vol. 81, no. 12, pp. 1687–1706, Dec. 1993.

[2] R. Soref, “Silicon photonics technology: past, present and future,” *Proc. SPIE*, vol. 5730, pp. 19-28, 2005.

[3] L. B. Soldano and E. C. M. Pennings, “Optical multi-mode interference devices based on self-imaging: principles and applications,” *J. Lightwave Technol.*, vol. 13, no. 4, p.615-627, Apr. 1995.

[4] D. S. Levy, K. H. Park, R. Scarmozzino, R. M. Osgood, C. Dries, P. Studenkov, and S. Forrest, “Fabrication of ultracompact 3-dB 2x2 MMI power splitters,” *IEEE Photon. Technol. Lett.*, vol. 11, no. 8, pp. 1009-1011, Aug. 1999.

[5] O. Bryngdahl, “Image formation using self-imaging techniques,” *J. Opt. Soc. Am.*, vol. 63, no. 4, pp. 416-419, Apr. 1973.

[6] R. Ulrich and G. Ankele, “Self-imaging in homogeneous planar optical waveguides,” *Appl. Phys. Lett.*, vol. 27, no. 6, pp. 337-339, Sept. 1975.